Journal of Inorganic and General Chemistry
ZAAC
Zeitschrift für anorganische und allgemeine Chemie
DOI: 10.1002/zaac.202100063
ARTICLE

Syntheses, Structures, and Bioactivity Evaluation of some Transition Metal Complexes with Aroylbis(*N*,*N*-diethylthioureas) Derived from Natural Compounds

Chien Thang Pham,[a] Thu Thuy Pham,[a] Viet Ha Nguyen,[b] Thi Nguyet Trieu,*[a] and Hung Huy Nguyen*[a]

Two novel benzoylthioureas derived from gallic acid, (tri-*O*-acetyl)galloyl-*N*,*N*-diethylthiourea **HL**^{1}, and cinnamic acid, cinnamoyl-*N*,*N*-diethylthiourea **HL**^{2} have been successfully prepared and characterized by means of elemental analysis, IR, NMR, high-resolution MS, and X-ray crystallography. The organic ligands react with $Ni(AcO)_2$ and $Cu(AcO)_2$ in MeOH under formation of *bis*-complexes with the compositions of $[M(L)_2]$ ($M{=}Ni^{2+}$, Cu^{2+}; $L{=}L^1$, L^2). Similar reactions with $Co(AcO)_2$, however, result in Co(III) *tris*-complexes $[Co(L)_3]$ ($L{=}L^1$, L^2) with the metal ions oxidized presumably by atmospheric dioxygen. X-ray crystallography and spectroscopic characterization reveal a *cis* square-planar coordination in the *bis*-complexes and *facial* octahedral geometry in the *tris*-complexes. In all of metal complexes, the deprotonated organic compounds ($\{L^1\}^-$ and $\{L^2\}^-$) serve as (*S*,*O*)-bidentate ligands. The ligand **HL**^{1} and its Ni(II) and Cu(II) complexes exhibit weak antiproliferative effects on the human MCF7 breast and HepG2 liver cancer cells with IC_{50} values in the range of 60–115 μM. Surprisingly, the *tris*-complex $[Co(L^1)_3]$ exhibits high cytotoxicity with IC_{50} values of 22.23 ± 1.58 μM for MCF7 and 28.30 ± 3.09 μM for HepG2 cancer cells. The activity against MCF7 cells is even more than that of cisplatin under the same conditions.

Introduction

It is widely known that since long ago, plants and herbs have been used through the world as food supplements and drugs for traditional medicine.[1] Nowadays, such natural products have been the basis of not only treatment of various diseases, but also the modern medicine and drug therapeutics.[2] Natural products display enormous structural diversity as well as molecular and pharmaceutical characteristics, which can be advantages in drug discovery.[3] A great number of medicines are developed either in the form of pharmacologically active natural products or semisynthetic derivatives.[1b,4] Besides organic derivatization, another potential approach to derive natural products is allowing them to bind with metal ions to form coordination compounds. This modification will affect structural and electronic features of the organic frameworks, which in turn will cause alteration in physiochemical as well as biomedicinal properties. Deliberate combination of metals with biologically active natural products may produce new compounds with even better biological activities.[5] Furthermore, higher stability of resulting metal complexes compared with the parent organic ligands could overcome the disadvantage of rapid degradation in clinical applications.[5b]

Gallic acid and cinnamic acid (Figure 1) are common natural phenolic acids found in free form or as derivatives in a wide variety of plants and food sources. Over the past few decades, a large number of research explorations have illustrated numerous biological activities of the phenolic acids and their derivatives, including antioxidant, antibacterial, anti-fungal, antiviral, anti-inflammatory and anticancer.[6]

Benzoyl(*N*,*N*-dialkylthioureas) **HL**^{0} are known as versatile ligands which can form stable complexes with various transition metal ions. In the majority of structurally characterized complexes, the ligands predominantly serve as monoanionic, bidentate (*S*,*O*)-chelators (Figure 2).[7] In addition to the wide spectrum of compositions and structures, benzoylthioureas and their transition metal complexes have been demonstrated potential applications in various fields such as catalysts, materials, metal extractions and pharmaceutical discovery.[8]

Taking into consideration the diverse structures and bioactivities of benzoylthiourea complexes and the considered phenolic acid derivatives, the combination of such two

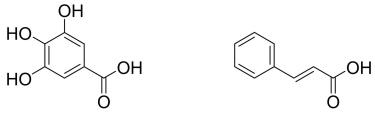

Gallic acid Cinnamic acid

Figure 1. Natural phenolic acids considered in this work.

[a] *Prof. Dr. C. Thang Pham, T. Thuy Pham, Prof. Dr. T. Nguyet Trieu, Prof. Dr. H. Huy Nguyen*
Department of Inorganic Chemistry
VNU University of Science, Vietnam National University, Hanoi
19 Le Thanh Tong, Hoan Kiem, 10021 Hanoi, Vietnam
E-mail: nguyenhunghuy@hus.edu.vn
trieuthinguyet@hus.edu.vn
[b] *V. Ha Nguyen*
Faculty of Education
Hanoi Metropolitan University
98 Duong Quang Ham, Cau Giay, 11306 Hanoi, Vietnam

Supporting information for this article is available on the WWW under https://doi.org/10.1002/zaac.202100063

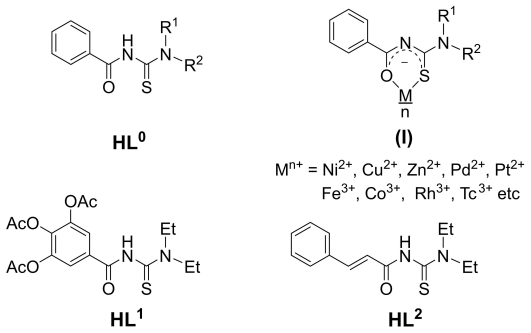

Figure 2. Benzoyl(*N*,*N*-dialkylthioureas) **HL⁰**, the predominant coordination mode **(I)** and the ligands used in this work **HL¹** and **HL²**.

components could give access to tuning a great number of biologically and pharmaceutically active compounds. Surprisingly, a survey of literature reveals only a few reports on synthesis and characterization of some benzoylthioureas derived from *O*-methylated gallic acid and the related metal complexes.[7i,9] None of these works provides structures of the obtained complexes.

As part of our ongoing effort to explore the coordination chemistry and bioactivity of benzoylthioureas derived from natural compounds, we report herein the syntheses, structures and *in vitro* anticancer activities against human MCF7 and HepG2 cancer cells of several metal complexes of two new ligands (tri-*O*-acetyl)galloyl-*N*,*N*-diethylthiourea **HL¹** and cinnamoyl-*N*,*N*-diethylthiourea **HL²** (Figure 2) with Ni^{2+}, Cu^{2+} and Co^{3+}.

Results and Discussion

The ligands HL¹ and HL²

The ligands **HL¹** and **HL²** were synthesized in good yields following reported procedures.[10] The synthesis of **HL¹** starts with the *O*-acetylation of gallic acid using acetic anhydride. Then, the acetylated acid is refluxed in an excess of $SOCl_2$ to convert into the corresponding acyl chloride. The reaction of the acyl chloride with *N*,*N*-diethylthiourea in dry THF with the presence of a stoichiometric amount of the supporting base Et_3N gives rise to **HL¹** in 60% yield (Scheme 1a). **HL²** can be

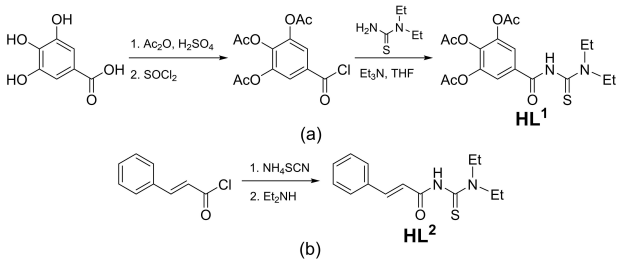

Scheme 1. Syntheses of the ligands (a) **HL¹** and (b) **HL²**.

prepared from a two-step, one-pot synthesis starting from commercially available starting materials, namely cinnamoyl chloride, NH_4SCN, and diethylamine (Scheme 1b). The pure ligand is obtained with 62% yield.

The results of elemental analyses and the existence of the molecular ions $[HL^1+H]^+$ or $[HL^2+H]^+$ in mass spectra are indicative for the expected compositions of the ligands. The IR spectra of **HL¹** and **HL²** show characteristic strong absorptions near 1660 cm^{-1}, which can be attributed to ketone ν_{CO} stretches. The additional strong absorption at 1769 cm^{-1} in the spectrum of **HL¹** is assigned to ester ν_{CO} stretches. In addition to the characteristic C=O bands, broad absorptions in the region above 3100 cm^{-1} indicate the presence of NH groups in the organic compounds, which is confirmed by broad singlet signals around 8.5 ppm in the ^1H NMR spectra of the ligands in $CDCl_3$. Signal belonging to the protons of the phenyl rings are detected in the range of 7.2–7.7 ppm. The CH_2 groups show two separate signals in the region of 3.0–4.0 ppm. This feature reflects hindered rotation around the C(S)–NEt_2 bond due to the partial multiple-bond character, which is frequently observed for benzoylthioureas.[7g,8a,11] This structural aspect also influences the resonance of the CH_3 protons in **HL¹**, which is found as two most upfield signals. In contrast to this well separation, only one broad singlet signal corresponds to the CH_3 groups in **HL²**. Besides mutual details, the ^1H NMR spectra also reveal characteristic structural features of each ligand. In particular, the resonances of the acetyl protons in **HL¹** are detected as a multiplet in the range of 2.33–2.35 ppm. The resonance of protons in the aliphatic double bond in **HL²** appears as two doublets at 7.68 ppm and 6.68 ppm with the typical *trans* vicinal spin coupling constant of 15.5 Hz. The $^{13}C\{^1H\}$ NMR spectra of the ligands strongly support their expected structures. The resonance of each CH_2 and CH_3 carbon atom of the peripheral ethyl residues appears as two separate signals in the upfield regions around 50 ppm and 10 ppm, respectively. The signals around 20 ppm in the spectrum of **HL¹** are assigned to the CH_3 carbon atoms of the acetyl groups, while the chemical shifts of the corresponding C=O groups occur about 165 ppm. In both ligands, the C=O and C=S carbon atoms of benzoylthiourea moieties give weak resonance signals near 178 ppm and 163 ppm, respectively. The aromatic carbon atoms of **HL¹** show resonances in the range of 120–150 ppm, while those of **HL²** appear in the region between the two signals assignable to carbon atoms of the aliphatic double bond at 144.0 ppm and 127.7 ppm.

Single crystals of the ligand **HL²** suitable for X-ray diffraction were obtained by slow evaporation of its MeOH/water solution. The compound crystallizes in the monoclinic space group $P2_1/c$ with two crystallographically independent molecules in the asymmetric unit (Figure 3). Selected bond lengths are listed in Table 1. The ligand **HL²** has a non-planar structure with carbonyl and thiocarbonyl groups in virtually opposite orientations. Such conformation is normally observed for other aroyl-(*N*,*N*-disubstituted)thioureas.[8d] The *N*,*N*-diethylthiourea groups are twisted from the corresponding cinnamoyl moieties with the angles of 63.17(5)° and 60.45(9)° between the mean least-square planes formed by the NC(S)N unit of the thiourea substituents and the

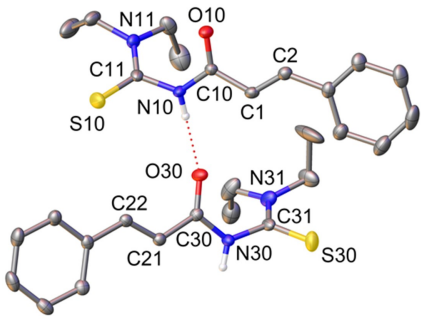

Figure 3. Molecular structure of the asymmetric unit of $(HL^2)_2$. Hydrogen atoms bonded to carbons are omitted for clarity. The dashed line presents the hydrogen bond.

Table 1. Selected bond length/Å in the unit $(HL^2)_2$.

Bond lengths/Å			
C10–O10	1.240(3)	C30–O30	1.236(3)
C10–N10	1.369(3)	C30–N30	1.376(3)
C11–N10	1.424(3)	C31–N30	1.420(3)
C11–N11	1.336(3)	C31–N31	1.328(3)
C11–S10	1.660(2)	C31–S30	1.672(2)
C1–C2	1.331(3)	C21–C22	1.327(3)

aroyl moieties. The C–O, C–S and C–N bond lengths resemble those in analogous aroy(*N*,*N*-disubstituted)thioureas (Table 1).[12] The partial double bond character of C(S)–NEt_2 distances is a confirmation of the hindered rotation around these bonds, which is detected in the NMR spectra. The supramolecular structure of HL^2 is stabilized by the intermolecular C=O···HN hydrogen bonds and π-π stacking (Figure S29).

The bis-complexes $[M(L)_2]$ ($M=Ni^{2+}$, Cu^{2+}; $L=L^1$, L^2)

Two equivalents of the ligands HL^1 or HL^2 readily react with one equivalent of $Ni(AcO)_2$ or $Cu(AcO)_2$ in MeOH in the presence of a weak base like NaAcO. Pure products directly deposited from the corresponding reaction mixtures. The chemical compositions of $[M(L)_2]$ ($M=Ni^{2+}$, Cu^{2+}; $L=L^1$, L^2) are confirmed by the results of the elemental analyses and the presence of peaks associated with the expected molecular ions $[M(L)_2+H]^+$ in the high resolution mass spectra. In the IR spectra of the complexes, the absence of broad absorptions in the region above 3100 cm^{-1} assigned to ν_{NH} stretches suggests the successful deprotonation of the ligands during complexation. In contrast to modest shifts of about 30 cm^{-1} of the carbonyl C=O bands in complexes derived from HL^2, such characteristic bands in complexes based on HL^1 show remarkable bathochromic shifts of approximately 140 cm^{-1}, which are clear evidence for the formation of the chelating (*S*,*O*)-benzoylthiourea. These structural features in the Ni(II) complexes are also observed in the NMR spectra, in particular, the disappearance of the broad singlet signal of the NH proton and the downfield shift of C=O signal with respect to the uncoordinated ligands. Additionally, the well-resolved splitting pattern of signals associated with ethyl residues in ^1H NMR spectrum of $[Ni(L^1)_2]$ reveals an increase in rotation barrier around C(S)-NEt_2 bonds. Furthermore, the NMR spectra of the Ni(II) complexes strongly reflect their diamagnetism, thereby pointing out the square planar coordination geometry of the Ni atoms. The structural conclusions drawn from spectroscopic studies are verified by X-ray diffraction analyses. Figure 4 presents the molecular structures of the compounds $[Cu(L^1)_2]$ and $[Cu(L^2)_2]$. Because the structure of the Ni(II) complex $[Ni(L^1)_2]$ is virtually identical with that of $[Cu(L^1)_2]$, no extra Figure is shown here. Selected bond lengths and angles are given in Table 2. The $[M(L^1)_2]$ ($M=Ni^{2+}$, Cu^{2+})

Table 2. Selected bond lengths/Å and bond angles/° in $[M(L^1)_2]$ ($M=Ni^{2+}$, Cu^{2+}) and $[Cu(L^2)_2]$.

Bond lengths/Å	$[Ni(L^1)_2]$	$[Cu(L^1)_2]$		$[Cu(L^2)_2]$
M–O10	1.8613(17)	1.9262(17)	Cu–O10/ Cu–O30	1.9157(14)/1.9248(13)
M–S10	2.1514(7)	2.2360(7)	Cu–S10/ Cu–S30	2.2334(6)/2.2357(7)
C10–O10	1.268(3)	1.263(3)	C10–O10/ C30–O30	1.258(2)/1.259(2)
C10–N10	1.313(3)	1.312(3)	C10–N10/ C30–N30	1.336(2)/1.340(2)
N10–C11	1.348(3)	1.351(3)	N10–C11/ N30–C31	1.343(2)/1.343(2)
C11–S10	1.734(2)	1.729(2)	C11–S10/ C31–S30	1.7415(17)/ 1.7427(18)
C11–N11	1.336(3)	1.339(3)	C11–N11/ C31–N31	1.345(2)/ 1.341(2)
Bond angles/°	$[Ni(L^1)_2]$	$[Cu(L^1)_2]$		$[Cu(L^2)_2]$
O10–M–S10	95.43(6)	93.97(6)	O10–Cu–S10/ O30–Cu–S30	93.00(4)/ 93.56(4)
O10–M–S10^i	178.68(6)	178.26(6)	O10–Cu–S30/ O30–Cu–S10/	176.27(6)/ 176.18(5)

Symmetry operations used to generate equivalent atoms: ^{i}–x, y, –z+1/2.

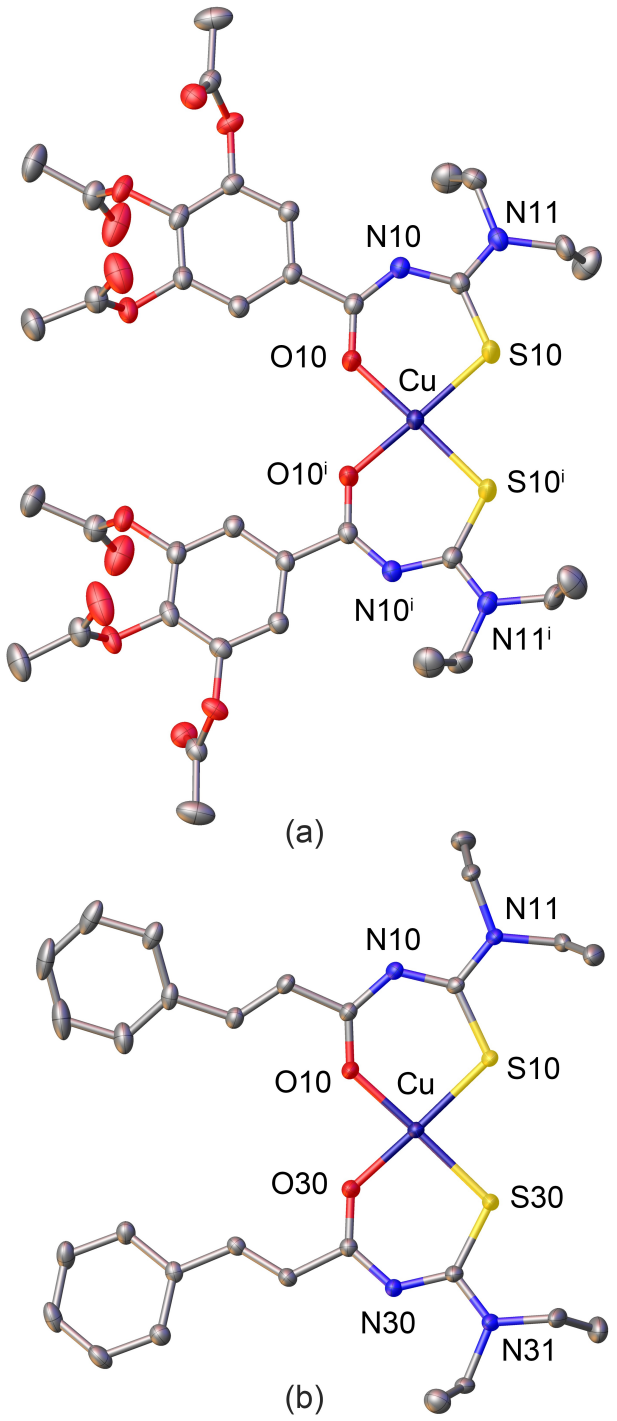

Figure 4. Molecular structures of the *bis* complexes (a) $[Cu(L^1)_2]$ and (b) $[Cu(L^2)_2]$. Symmetry operations used to generate equivalent atoms: ^{i} −x, y, −z+1/2. Hydrogen atoms are omitted for clarity.

complexes crystallize isomorphic as dichloromethane solvates in the monoclinic space group *C2/c* with a half unit of $[M(L^1)_2]\cdot CH_2Cl_2$ in the asymmetric unit. For the $[M(L^2)_2]$ series, we could only successfully crystallize the $[Cu(L^2)_2]$ complex, which crystallizes in the solvent-free form in the triclinic space group *P-1* with one molecule in the asymmetric unit. The structural determination indicates mononuclear square planar complexes with *cis* configuration, in which divalent metal ions are coordinated by two deprotonated ligands $\{L^1\}^-$ or $\{L^2\}^-$ through two (*S*,*O*)-chelates. Such bidentate *cis*-L(*S*,*O*) coordination which is more thermodynamically favorable than *trans*-L(*S*,*O*) fashion, has been observed in majority of reported benzoylthiourea complexes with divalent metal ions.[8c,13] The M–O and M–S bond lengths ($M=Ni^{2+}$, Cu^{2+}) are in the same ranges as those found in the analogous complexes with other benzoylthiourea ligands.[7b,c,h,14] The planarity of the six-membered chelate rings as well as the partial double bond character C–S, C–O and C–N bonds in all complexes (Table 2) is in line with the well-known extended π-systems in chelating benzoylthiourea moieties.[7g]

In comparison to the counterparts in the uncoordinated ligand **HL²**, the elongation of the C–O and C–S bonds and the contraction of the C–N distances within the chelate rings in the structure of the complex $[Cu(L^2)_2]$ strongly suggest the higher delocalization of π-electrons within the thiourea moieties by the complexation.

The tris-complexes [Co(L)₃] (L = L¹, L²)

The *tris*-complexes $[Co(L)_3]$ ($L=L^1$, L^2) are readily formed in the reaction of $Co(AcO)_2$ (1 equiv.) with the corresponding organic ligands (3 equiv.) in MeOH. Addition of a weak base like NaAcO could accelerate the complex formation. The color change of the reaction mixture is a visible sign of the oxidation of Co(II) ions probably by atmospheric dioxygen during the complexation. Similar redox reactions have been reported in the preparation of Co(III) *tris*-complexes with other benzoylthiourea ligands.[15] The result of elemental analysis and the presence of the predicted ions $[Co(L^1)_3+H]^+$ and $[Co(L^2)_3+Na]^+$ in the mass spectra confirm the chemical composition of the neutral *tris*-complexes. In their IR spectra, the disappearance of the broad absorption in the region above 3100 cm^{-1} and the bathochromic shift of the intense absorption corresponding to the ketone $\nu_{C=O}$ vibrations illustrate the successful deprotonation of the ligand and the chelate formation with π-electron delocalization. The formal oxidation state "+3" of the cobalt ion is validated by the diamagnetism of the products. It comes as no surprise that the ^{1}H NMR spectra measured in $CDCl_3$ show no signal accounting for NH proton in the downfield region 8.0–9.0 ppm, which confirms the deprotonation of the ligands. Similarly to the situation in the complex $[Ni(L^1)_2]$, a considerable increase of the rotational barrier around C(S)–NEt_2 bonds upon coordination is observed in the ^{1}H NMR spectra of both Co(III) complexes. By comparison with the simple splitting patterns of the same protons in the uncoordinated ligands and in the Ni(II) complexes, the more delicate fine structures of the CH_2 protons of the ethyl residues presumably resulting from geminal and vicinal couplings in combination with the overlap of resulting signals apparently reflect the substantial increase of rigid arrangement around the tertiary nitrogen atoms.[16] In contrast to the complexity of ^{1}H NMR spectra, the $^{13}C\{^1H\}$ NMR spectra are straightforward. Except the significant downfield shifts of

the resonance for carbonyl C=O groups because of the coordination with the Co(III) ions, the $^{13}C\{^1H\}$ NMR spectra of the complexes and the free ligands closely resemble. The structures elucidated using the spectroscopic data are confirmed by X-ray structure determination. Figure 5 depicts the structures of the complexes, and selected structural parameters are listed in Table 3.

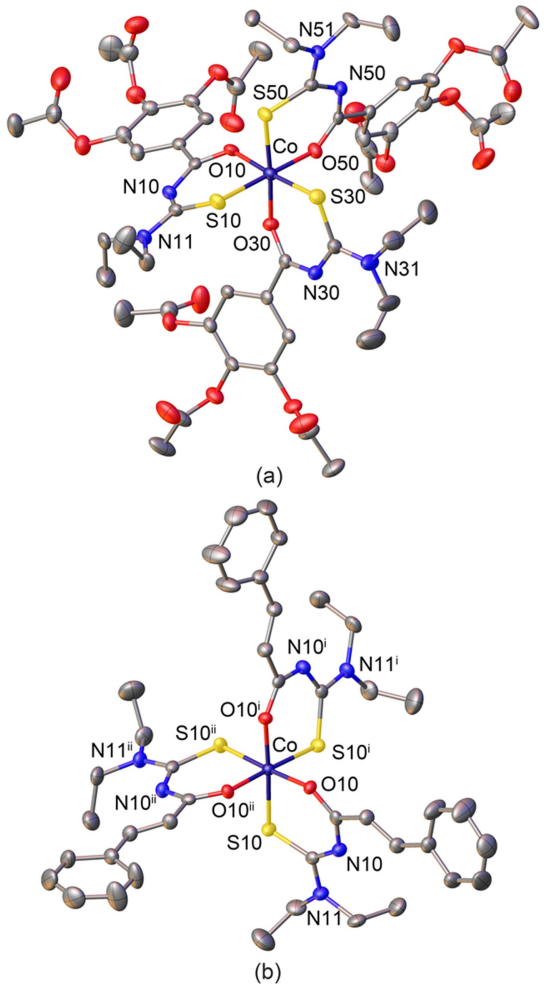

Figure 5. Molecular structure of the *tris* complexes (a) $[Co(L^1)_3]$ and (b) $[Co(L^2)_3]$. Symmetry operations used to generate equivalent atoms: [i] 1−y, x−y, z and [ii] 1+y−x, 1−x, z. Hydrogen atoms are omitted for clarity.

The complex $[Co(L^1)_3]$ crystallizes in the solvent-free form in the triclinic space group *P-1* with one molecule in the asymmetric unit. Whereas the remaining complex crystallizes in the solvated form in the non-centrosymmetric trigonal space group *R3* with one-third unit of $[Co(L^2)_3]\cdot CH_2Cl_2$ in the asymmetric unit, in which a crystallographic C_3-axis passes through the Co atom and the carbon atom of the co-crystalized solvent molecule. The complexes are mononuclear with Co(III) ions octahedrally coordinated by three deprotonated (*S*,*O*)-bidentate ligands $\{L^1\}^-$ or $\{L^2\}^-$ with a *facial* arrangement of donor atoms. Hitherto, this type of arrangement is the unique coordination geometry known for homoleptic *tris*-complexes of benzoylthioureas and trivalent metal ions.[13] The Co–O and Co–S bond lengths are in the range of 1.915(2)–1.936(4) Å and 2.2034(9)–2.2120(2) Å, respectively. This is in good agreement with the values observed in the Co(III) *tris*-complexes with other benzoylthioureato ligands.[15,17] The planarity of chelate rings and the partial double bond character of the C–O, C–N, and C–S bonds within the benzoylthiourea moieties imply the existence of typical extended π-systems, which are detected in the IR spectra. In the supramolecular structure of $[Co(L^1)_3]$, two neighboring structural units interact with each other by a π–π stacking (Figure S30).

Anticancer activity studies

Recent literature reviews witness wide spectrum of bioactivities of aroyl/acylthiourea ligands and their transition metal complexes.[8b–d] However, there are only several reports on antitumor activities of this family of ligands,[18] and their homoleptic complexes.[18a,19] In the present study, antiproliferative effects of the ligands and their metal complexes on human MCF7 breast and HepG2 liver cancer cells were inspected using dose-response assays. Table 4 lists the IC_{50}

Table 3. Selected bond lengths/Å and bond angles/° in $[Co(L^1)_3]$ and $[Co(L^2)_3]$.

Bond lengths/Å							
$[Co(L^1)_3]$						$[Co(L^2)_3]$	
Co–O10	1.936(4)	Co–O30	1.924(4)	Co–O50	1.918(4)	Co–O10	1.915(2)
Co–S10	2.2120(2)	Co–S30	2.206(2)	Co–S50	2.2047(2)	Co–S10	2.2034(9)
C10–O10	1.259(7)	C30–O30	1.269(7)	C50–O50	1.265(7)	C10–O10	1.267(4)
C10–N10	1.327(7)	C30–N30	1.327(8)	C50–N50	1.316(7)	C10–N10	1.327(4)
N10–C11	1.343(8)	N30–C31	1.350(8)	N50–C51	1.357(7)	N10–C11	1.337(4)
C11–S10	1.730(7)	C31–S30	1.732(7)	C51–S50	1.725(6)	C11–S10	1.726(3)
C11–N11	1.349(7)	C31–N31	1.318(8)	C51–N51	1.344(7)	C11–N11	1.341(4)
Bond angles/°							
$[Co(L^1)_3]$						$[Co(L^2)_3]$	
O10–Co–S10	93.03(13)	O30–Co–S30	96.32(13)	O50–Co–S50	92.83(13)	O10–Co–S10	94.24(7)
O10–Co–S30	176.16(13)	O30–Co–S50	175.88(14)	O50–Co–S10	177.59(14)	O10–Co–S10[ii]	176.98(7)

Symmetry operations used to generate equivalent atoms: [ii] 1+y−x, 1−x, z.

Table 4. IC_{50} values/μM of the ligands and complexes.

Tested compounds	MCF7	HepG2	Tested compounds	MCF7	HepG2
HL^1	70.17 ± 5.80	97.63 ± 9.65	**HL**^{2}	> 380	> 380
$[Ni(L^1)_2]$	64.84 ± 6.94	89.42 ± 2.20	$[Ni(L^2)_2]$	> 170	> 170
$[Cu(L^1)_2]$	94.21 ± 2.46	113.2 ± 1.14	$[Cu(L^2)_2]$	> 170	> 170
$[Co(L^1)_3]$	22.23 ± 1.58	28.30 ± 3.09	$[Co(L^2)_3]$	> 100	> 100
cisplatin[20]	45.7 ± 1.2	13.3 ± 1.1			

values obtained and that of cisplatin determined under the same condition.[20]

The results indicate that the ligand **HL**^{1} and its complexes cause remarkable antiproliferative effects on the two tested cell lines, while the remaining compounds have almost no activity against the cancer cells. Although **HL**^{1} and its Ni(II) and Cu(II) complexes (IC_{50} values > 50 μM) show weak growth inhibition for both HepG2 and MCF7 cancer cells, the IC_{50} values are comparable with those of some aroylthioureas,[18c,d] and similar homoleptic complexes tested against the same cell lines (Figure 6).[19e,g] Surprisingly, the *tris*-complex $[Co(L^1)_3]$ exhibits high cytotoxicity. The activity against MCF7 cells is even more than that of cisplatin under the same experimental condition. In comparison with IC_{50} values of the uncoordinated ligand, those of the Co(III) complex decrease by a factor about 3.5. The enhanced activities of the Co(III) complex with respect to the uncoordinated ligand **HL**^{1} indicate the synergistic effect of metal ion.[5a,21]

Conclusions

Two new benzoylthioureas bearing natural compounds derived moieties, namely gallic acid, **HL**^{1}, and cinnamic acid, **HL**^{2}, have been synthesized and examined for their coordination potential with Ni^{2+}, Cu^{2+} and Co^{3+} ions. In all complexes, the ligands act as monoanionic chelators with the (*S*,*O*) donor sets and selectively form *cis* square planar and *facial* octahedral complexes with di- and tri-valent metal ions, respectively. Anticancer activity studies demonstrate that the ligand **HL**^{1} and its Ni(II) and Cu(II) complexes show weak growth inhibition of the human MCF7 breast and HepG2 liver cancer cells, while the corresponding Co(III) complex presents considerable antiproliferative effects against the two tested cancer cell lines. Its cytotoxicity against MCF7 cells even more than that of cisplatin under the same condition.

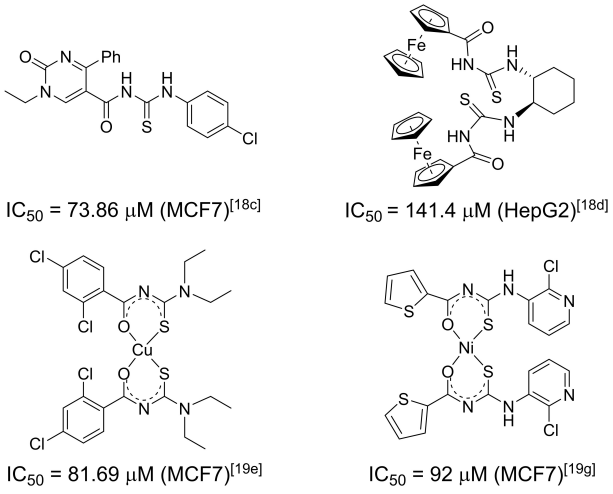

Figure 6. Structures and IC_{50} values of some aroylthioureas and homoleptic complexes previously reported.

Experimental Section

Materials: All chemicals used in this study were reagent grade and used without further purification. Solvents were dried and used freshly distilled unless otherwise stated.

Physical Measurements: Infrared spectra were measured as KBr pellets on an Affinity-1S FTIR-spectrometer between 400 and 4000 cm^{-1}. NMR spectra were taken with an AscendTM 500 MHz (Bruker) multinuclear spectrometer. ESI high resolution mass spectra were measured with an LTQ Orbitrap XLTM and SCIEX X500 QTOF instruments. All MS results are given in the form: *m*/*z*, assignment. Elemental analyses of carbon, hydrogen, nitrogen and sulfur were determined using a Heraeus (Germany) vario EL elemental analyzer. Reproductions of the IR, NMR and MS spectra are given as Supplementary Material.

Synthesis of the ligand HL^1: The ligand was synthesized following the method reported by Dixon and Taylor with some modifications.[10a] A mixture of the anhydrous acetylated gallic acid (3.40 g, 0.02 mol) prepared according to the procedure adapted from Ye et al.[22] and an excess amount of $SOCl_2$ (15 mL, 0.2 mol) was heated at 80 °C under nitrogen atmosphere for 3 h to obtain a clear solution. After that, the residual $SOCl_2$ was removed under reduced pressure. The resulting solid was dissolved in dry THF (50 mL) and then added dropwise to a mixture of *N*,*N*-diethylthiourea (2.64 g, 0.02 mol) and Et_3N (6.4 mL, 0.02 mol) in dry THF (20 mL). The reaction mixture was heated up to 40–50 °C and stirred for 2 h. After cooling, the mixture to room temperature, a colorless precipitate of $Et_3N{\cdot}HCl$ was filtered off, and THF was removed under low pressure. The obtained solid was washed with MeOH to give the HL ligand as a colourless solid. Yield: 60 % (4.93 g). Elemental analysis Calcd. for $C_{18}H_{22}O_7N_2S$: C, 52.67; H, 5.40; N, 6.83; S, 7.81 %. Found: C, 52.48; H, 5.57; N, 6.65; S, 7.65 %. IR (KBr, cm^{-1}): 3234 (w), 2974 (w), 2934 (w), 1769 (s), 1663 (m), 1528 (m), 1468 (m), 1423 (s), 1369 (s), 1329 (m), 1285 (m), 1204 (s), 1186 (s), 1167 (s), 1126 (s) 1059 (s), 1013 (s), 897 (m), 878 (m), 856 (w), 760 (w), 698 (w), 604 (w), 557 (w), 415 (w). ^{1}H NMR (500 MHz, $CDCl_3$, *ppm*): 8.32 (br, s, 1H, NH), 7.66 (s, 2H, Ph), 4.05 (br, s, 2H, CH_2), 3.60 (br, s, 2H, CH_2), 2.35–2.33 (br, m, 9H, CH_3COO), 1.39 (br, s, 3H, CH_3), 1.32 (br, s, 3H, CH_3). $^{13}C\{^1H\}$ NMR ($CDCl_3$, *ppm*): 178.7 (CS), 167.6 (*m*-CH_3COO), 166.4 (*p*-CH_3COO), 161.5 (CO), 143.8, 138.4, 130.8, 120.5 (Ph), 48.0, 47.7 (CH_2),

20.6 (*m*-CH_3COO), 20.2 (*p*-CH_3COO), 13.3, 11.4 (CH_3). +ESI MS (*m/z*): 411.1219 (calcd. 411.1226), 100% $[HL^1+H]^+$.

Synthesis of the ligand HL^2: The ligand was synthesized following the standard procedure proposed by Douglass and Dain.[10b] To a suspension of NH_4SCN (1.52 g, 0.02 mol) in 20 mL dry acetone was added dropwise solution of cinnamoyl chloride (3.33 g, 0.02 mol) in 20 mL dry acetone. The reaction mixture was then heated up to 50 °C and stirred for 1 h. After cooling the mixture to room temperature, 20 mL dry acetone containing diethylamine (2.1 mL, 0.02 mol) were added dropwise. After that, the reaction mixture was refluxed for 2 h and then poured into 500 mL water with vigorous stirring. The isolated solid was collected by filtration and washed with water. Recrystallization of the obtained pale-yellow solid from hot MeOH and water afforded the ligand as a colorless solid. Yield: 62% (3.25 g). Elemental analysis Calcd. for $C_{14}H_{18}ON_2S$: C, 64.09; H, 6,92; N, 10.68; S, 12.22%. Found: C, 63.94; H, 7.12; N, 10.46; S, 11.96%. IR (KBr, cm^{-1}): 3250 (w), 2976 (w), 2935 (w), 1665 (s), 1626 (s), 1531 (s), 1449 (s), 1421 (s), 1344 (s), 1283 (s), 1233 (s), 1192 (s), 1126 (s), 1072 (m), 1003 (s), 905 (w), 873 (w), 766 (s), 714 (m), 683 (m), 565 (m), 536 (m), 486 (m). ^{1}H NMR (500 MHz, $CDCl_3$, *ppm*): 8.77 (br, s, 1H, NH), 7.68 (d, $J=15.5$ Hz, 1H, *trans*-CH=CH), 7.54–7.52 (m, 2H, Ph), 7.39–7.38 (m, 3H, Ph), 6.68 (d, $J=15.5$ Hz, 1H, *trans*-CH=CH), 4.02 (br, s, 2H, CH_2), 3.63 (br, s, 2H, CH_2), 1.33 (br, s, 6H, CH_3). $^{13}C\{^1H\}$ NMR ($CDCl_3$, *ppm*): 179.2 (CS), 166.9 (CO), 144.0 (*trans*-CH=CH), 134.4, 129.2, 128.9, 128.2 (Ph), 127.7 (*trans*-CH=CH), 47.7, 44.6 (CH_2), 13.2, 13.0 (CH_3). +ESI MS (*m/z*): 263.1210 (calcd. 263.1218), 15% $[HL^2+H]^+$; 285.1027 (calcd. 285.1038), 100% $[HL^2+Na]^+$. Single crystals suitable for X-ray analysis were obtained by recrystallization of the compound from a mixture of MeOH and water.

Syntheses of $[M(L)_2]$ (M=Ni^{2+}, Cu^{2+}): $Ni(OAc)_2\cdot 4\ H_2O$ or $Cu(OAc)_2\cdot 2H_2O$ were dissolved in 1 mL of MeOH. The ligands HL^1 or HL^2 (0.2 mmol) were added and the reaction mixtures were kept stirring at 40 °C for 30 min before the addition of NaOAc (16.4 mg, 0.2 mmol). During an additional stirring at 40 °C for 1 h, the pure products deposited from the solution and were then collected by filtration, washed with cold MeOH and dried in vacuum.

Data for $[Ni(L^1)_2]$: Purple. Yield: 75% (65.8 mg). Elemental analysis Calcd. for $C_{36}H_{42}O_{14}N_4S_2Ni$: C, 49.27; H, 4.82; N, 6.38; S, 7.31%. Found: C, 49.03; H, 5.02; N, 6.17; S, 7.01%. IR (KBr, cm^{-1}): 2976 (w), 2934 (w), 1771 (s), 1528 (m), 1499 (s), 1418 (s), 1371 (s), 1279 (m), 1242 (m), 1180 (s), 1153 (s), 1076 (m), 1047 (s), 1009 (s), 899 (m), 847 (m), 800 (m), 762 (m), 735 (w), 664 (w), 586 (w), 550 (w), 501 (w), 415 (s). ^{1}H NMR (500 MHz, $CDCl_3$, *ppm*): 7.79 (s, 2H, Ph), 3.74 (q, $J=7.0$ Hz, 4H, CH_2), 2.28 (br, s, 3H, *p*-CH_3COO), 2.27 (br, s, 6H, *m*-CH_3COO), 1.27 (t, $J=7.0$ Hz, 3H, CH_3), 1.23 (t, $J=7.0$ Hz, 3H, CH_3). $^{13}C\{^1H\}$ NMR ($CDCl_3$, *ppm*): 172.8 (CS), 169.9 (CO), 167.8 (*m*-CH_3COO), 166.6 (*p*-CH_3COO), 142.8, 137.1, 135.2, 121.5 (Ph), 46.3, 45.8 (CH_2), 20.6 (*m*-CH_3COO), 20.2 (*p*-CH_3COO), 13.1, 12.5 (CH_3). +ESI MS (*m/z*): 877.1526 (calcd. 877.1571), 100% $[Ni(L^1)_2+H]^+$. Single crystals suitable for X-ray analysis were obtained by slow evaporation of a solution of the complex in a mixture of MeOH and CH_2Cl_2.

Data for $[Cu(L^1)_2]$: Brownish grey. Yield: 70% (61.8 mg). Elemental analysis Calcd. for $C_{36}H_{42}O_{14}N_4S_2Cu$: C, 49.00; H, 4.80; N, 6.35; S, 7.27%. Found: C, 48.72; H, 4.91; N, 6.08; S, 7.13%. IR (KBr, cm^{-1}): 2974 (w), 2936 (w), 1771 (s), 1543 (w), 1518 (m), 1495 (s), 1423 (s), 1371 (s), 1279 (m), 1238 (w), 1179 (s), 1153 (s), 1074 (m), 1045 (s), 1009 (s), 899 (m), 847 (m), 797 (m), 764 (m), 735 (w), 687 (w), 588 (w), 546 (m), 486 (m), 415 (s). +ESI MS (*m/z*): 904.1334 (calcd. 904.1333), 100% $[Cu(L^1)_2+Na]^+$; 882.1552 (calcd. 882.1513), 25% $[Cu(L^1)_2+H]^+$. Single crystals suitable for X-ray analysis were obtained by slow evaporation of a solution of the complex in a mixture of MeOH and CH_2Cl_2.

Data for $[Ni(L^2)_2]$: Reddish brown. Yield: 83% (48.1 mg). Elemental analysis Calcd. for $C_{28}H_{34}O_2N_4S_2Ni$: C, 57.84; H, 5.89; N, 9.64; S, 11.03%. Found: C, 57.97; H, 5.72; N, 9.58; S, 10.91%. IR (KBr, cm^{-1}): 2978 (w), 2932 (w), 1634 (m), 1489 (s), 1408 (s), 1352 (s), 1296 (m), 1260 (m), 1236 (m), 1184 (m), 1128 (m), 1076 (m), 1016 (m), 989 (w), 879 (w), 760 (m), 713 (w), 683 (m), 600 (w), 488 (w). ^{1}H NMR (500 MHz, $CDCl_3$, *ppm*): 7.65 (d, $J=11.0$ Hz, 1H, *trans*-CH=CH), 7.57–7.38 (m, 5H, Ph), 6.61 (d, $J=11.0$ Hz, 1H, *trans*-CH=CH), 3.77 (br, s, 4H, CH_2), 1.29 (br, s, 3H, CH_3), 1.24 (br, s, 3H, CH_3). $^{13}C\{^1H\}$ NMR ($CDCl_3$, *ppm*): 173.1 (CS), 172.0 (CO), 140.8 (*trans*-CH=CH), 135.7, 129.2, 128.7, 127.9 (Ph), 127.2 (*trans*-CH=CH), 45.9, 45.2 (CH_2), 13.1, 12.6 (CH_3). +ESI MS (*m/z*): 603.1382 (calcd. 603.1374), 14% $[Ni(L^2)_2+Na]^+$; 581.1538 (calcd. 581.1555), 75% $[Ni(L^2)_2+H]^+$; 285.1013 (calcd. 285.1038), 100% $[HL^2+Na]^+$.

Data for $[Cu(L^2)_2]$: Brownish grey. Yield: 75% (43.9 mg). Elemental analysis Calcd. for $C_{28}H_{34}O_2N_4S_2Cu$: C, 57.36; H, 5.85; N, 9.56; S, 10.94%. Found: C, 57.54; H, 5.67; N, 9.38; S, 10.78%. IR (KBr, cm^{-1}): 2968 (w), 2932 (w), 1634 (m), 1512 (s), 1491 (s), 1412 (s), 1352 (m), 1294 (w), 1260 (w), 1176 (w), 1128 (w), 1070 (w), 1011 (w), 972 (w), 768 (w), 687 (w), 588 (w), 548 (w). +ESI MS (*m/z*): 608.1334 (calcd. 608.1317), 12% $[Cu(L^2)_2+Na]^+$; 586.1496 (calcd. 586.1497), 42% $[Cu(L^2)_2+H]^+$; 285.1032 (calcd. 285.1038), 100% $[HL^2+Na]^+$. Single crystals suitable for X-ray analysis were obtained by slow evaporation of the filtrate.

Syntheses of $[Co(L)_3]$: HL^1 or HL^2 (0,3 mmol) were added to a solution of $Co(OAc)_2\cdot 4\ H_2O$ (25.0 mg, 0.1 mmol) in MeOH (1 mL). During stirring of reaction mixtures at room temperature for 15 min, the colour of the solutions changed gradually to green. After the addition of NaOAc (24.6 mg, 0.3 mmol), the reaction mixtures were stirred at 40 °C for 1 h. The final solution was slowly evaporated at room temperature. During this process, the pure products deposited as green solids, which were then filtered off, washed with cold MeOH and dried in vacuum.

Data for $[Co(L^1)_3]$: Yield: 70% (90.1 mg). Elemental analysis Calcd. for $C_{54}H_{63}O_{21}N_6S_3Co$: C, 50.39; H, 4.93; N, 6.53; S, 7.47%. Found: C, 50.12; H, 5.06; N, 6.28; S, 7.22%. IR (KBr, cm^{-1}): 2976 (w), 2932 (w), 1770 (s), 1530 (m), 1495 (s), 1406 (s), 1371 (s), 1354 (s), 1279 (m), 1238 (m), 1179 (s), 1155 (s), 1128 (s), 1045 (s), 1007 (s), 899 (m), 880 (m), 847 (m), 797 (w), 737 (w), 687 (w), 590 (w), 548 (w), 488 (w), 422 (w). ^{1}H NMR (500 MHz, $CDCl_3$, *ppm*): 7.91 (s, 2H, Ph), 3.86–3.73 (m, 4H, CH_2), 2.29 (s, 3H, *p*-CH_3COO), 2.27 (s, 6H, *m*-CH_3COO), 1.21 (t, $J=7.0$ Hz, 3H, CH_3). $^{13}C\{^1H\}$ NMR ($CDCl_3$, ppm): 174.8 (CS), 172.3 (CO), 167.7 (*m*-CH_3COO), 166.6 (*p*-CH_3COO), 142.6, 137.0, 136.9, 121.6 (Ph), 45.9, 45.8 (CH_2), 20.6 (*m*-CH_3COO), 20.2 (*p*-CH_3COO), 13.1, 12.8 (CH_3). +ESI MS (*m/z*): 1287.2653 (calcd. 1287.2619), 100% $[Co(L^1)_3+H]^+$. Single crystals suitable for X-ray analysis were obtained by slow evaporation of a solution of the complex in DMF.

Data for $[Co(L^2)_3]$: Yield: 88% (74.1 mg). Elemental analysis Calcd. for $C_{42}H_{51}O_3N_6S_3Co$: C, 59.84; H, 6.10; N, 9.97; S, 11.41%. Found: C, 59.67; H, 6.25; N, 9.82; S, 11.53%. IR (KBr, cm^{-1}): 2980 (w), 2930 (w), 1634 (s), 1510 (s), 1485 (s), 1422 (s), 1404 (s), 1350 (s), 1248 (m), 1190 (m), 1128 (m), 1072 (m), 1011 (m), 978 (m), 874 (w), 843 (w), 762 (m), 727 (w), 685 (w), 613 (w), 486 (w). ^{1}H NMR (500 MHz, $CDCl_3$, *ppm*): 7.71 (d, $J=16.0$ Hz, 1H, *trans*-CH=CH), 7.51 (s, 2H, Ph), 7.33–7.32 (m, 3H, Ph), 6.84 (d, $J=16.0$ Hz, 1H, *trans*-CH=CH), 3.95–3.77 (m, 4H, CH_2), 1.28 (br, s, 3H, CH_3), 1.20 (br, s, 3H, CH_3). $^{13}C\{^1H\}$ NMR ($CDCl_3$, ppm): 175.9 (CS), 174.2 (CO), 140.2 (*trans*-CH=CH), 136.1, 129.1, 128.9, 128.6 (Ph), 127.9 (*trans*-CH=CH), 45.5, 45.1 (CH_2), 13.3, 13.1 (CH_3). +ESI MS (*m/z*): 865.2479 (calcd. 865.2414), 63% $[Co(L^2)_3+Na]^+$. Single crystals suitable for X-ray analysis were obtained by slow evaporation of a solution of the complex in a mixture of MeOH and CH_2Cl_2.

X-ray crystallography: The intensities for the X-ray determinations of $[Co(L^1)_3]$, $[Ni(L^1)_2]\cdot CH_2Cl_2$, $[Cu(L^1)_2]\cdot CH_2Cl_2$, HL^2, $[Co(L^2)_3]\cdot CH_2Cl_2$ and $[Cu(L^2)_2]$ were collected on a Bruker D8 QUEST instrument at 170 K with Mo Kα radiation ($\lambda = 0.71073$ Å) using a TRIUMPH monochromator. Standard procedures were applied for data reduction and absorption correction.[23] Structure solution and refinement were performed with the SHELXT and SHELXL 2014/7 programs.[24] Hydrogen atoms were calculated for idealized positions and treated with the 'riding model' option of SHELXL. The program OLEX2-1.2 was used for the molecular representation.[25] More details on data collections and structure calculations are contained in Table S1. Crystallographic data for the structures in this paper have been deposited with the Cambridge Crystallographic Data Centre, CCDC, 12 Union Road, Cambridge CB21EZ, UK. Copies of the data can be obtained free of charge on quoting the depository numbers CCDC-1995471 $[Co(L^1)_3]$, CCDC-1995472 $\{[Ni(L^1)_2]\cdot CH_2Cl_2\}$, CCDC-1995473 $\{[Cu(L^1)_2]\cdot CH_2Cl_2\}$, CCDC-2055051 $(\mathbf{HL^2})_2$, CCDC-2055052 $\{[Co(L^2)_3]\cdot CH_2Cl_2\}$ and CCDC-2055053 $[Cu(L^2)_2]$ (Fax: +44-1223-336-033; E-Mail: deposit@ccdc.cam.ac.uk, http://www.ccdc.cam.ac.uk).

In vitro cell tests: The cytotoxic activity of the compounds was determined using a MTT assay. Human MCF-7 and HepG2 cancer cells were obtained from the American Type Culture Collection (Manassas, VA) ATCC. Cells were cultured in standard procedure using medium RPMI 1640 supplemented with 10% FBS (Fetal bovine serum), humidified atmosphere of 5% CO_2 at 37 °C. The 100 µL samples of the complexes with different concentration (in mixture of DMSO and cell culture medium) were added to the wells on 96-well plates. Cells were detached with trypsin and EDTA and seeded in each well with 3×10^4 cells per well. After incubation for 48 h, a MTT solution (20 µL, 4 mg·mL^{-1}) of phosphate buffer saline was added into each well. The cells were further incubated for 4 h to form purple formazan precipitate, which was separated by centrifugation and dissolved by adding DMSO (100 µL). The optical density of the solution was determined by a plate reader (TECAN) at 540 nm. The inhibition ratio was calculated on the basis of the optical densities obtained from three replicate tests.

Acknowledgements

This research is funded by Vietnam National Foundation for Science and Technology Development (NAFOSTED) under grant number 104.03-2016.48.

Keywords: Benzoylthiourea · Ni(II) complexes · Cu(II) complexes · Co(III) complexes · anticancer activities

[1] a) A. Gurib-Fakim, *Mol. Aspects Med.* **2006**, *27*, 1–93; b) G. A. Cordell, M. D. Colvard, *J. Nat. Prod.* **2012**, *75*, 514–525.
[2] a) C. Basmadjian, Q. Zhao, E. Bentouhami, A. Djehal, C. G. Nebigil, R. A. Johnson, M. Serova, A. de Gramont, S. Faivre, E. Raymond, L. G. Désaubry, *Front. Chem.* **2014**, *2(20)*, 1–18; b) A. G. Atanasov, B. Waltenberger, E.-M. Pferschy-Wenzig, T. Linder, C. Wawrosch, P. Uhrin, V. Temml, L. Wang, S. Schwaiger, E. H. Heiss, J. M. Rollinger, D. Schuster, J. M. Breuss, V. Bochkov, M. D. Mihovilovic, B. Kopp, R. Bauer, V. M. Dirsch, H. Stuppner, *Biotechnol. Adv.* **2015**, *33*, 1582–1614; c) D. J. Newman, G. M. Cragg, *J. Nat. Prod.* **2016**, *79*, 629–661.
[3] A. G. Atanasov, S. B. Zotchev, V. M. Dirsch, I. E. Orhan, M. Banach, J. M. Rollinger, D. Barreca, W. Weckwerth, R. Bauer, E. A. Bayer, M. Majeed, A. Bishayee, V. Bochkov, G. K. Bonn, N. Braidy, F. Bucar, A. Cifuentes, G. D'Onofrio, M. Bodkin, M. Diederich, A. T. Dinkova-Kostova, T. Efferth, K. El Bairi, N. Arkells, T.-P. Fan, B. L. Fiebich, M. Freissmuth, M. I. Georgiev, S. Gibbons, K. M. Godfrey, C. W. Gruber, J. Heer, L. A. Huber, E. Ibanez, A. Kijjoa, A. K. Kiss, A. Lu, F. A. Macias, M. J. S. Miller, A. Mocan, R. Müller, F. Nicoletti, G. Perry, V. Pittalà, L. Rastrelli, M. Ristow, G. L. Russo, A. S. Silva, D. Schuster, H. Sheridan, K. Skalicka-Woźniak, L. Skaltsounis, E. Sobarzo-Sánchez, D. S. Bredt, H. Stuppner, A. Sureda, N. T. Tzvetkov, R. A. Vacca, B. B. Aggarwal, M. Battino, F. Giampieri, M. Wink, J.-L. Wolfender, J. Xiao, A. W. K. Yeung, G. Lizard, M. A. Popp, M. Heinrich, I. Berindan-Neagoe, M. Stadler, M. Daglia, R. Verpoorte, C. T. Supuran, T. the International Natural Product Sciences, *Nature Reviews Drug Discovery* **2021**.
[4] C. Tringali, *Bioactive Compounds from Natural Sources: Natural Products as Lead Compounds in Drug Discovery*, 2nd Edition ed., CRC Press, Boca Raton, **2011**.
[5] a) S. Wanninger, V. Lorenz, A. Subhan, F. T. Edelmann, *Chem. Soc. Rev.* **2015**, *44*, 4986–5002; b) M. Pröhl, U. S. Schubert, W. Weigand, M. Gottschaldt, *Coord. Chem. Rev.* **2016**, *307*, 32–41.
[6] a) A. P. Subramanian, A. A. John, M. V. Vellayappan, A. Balaji, S. K. Jaganathan, E. Supriyanto, M. Yusof, *RSC Adv.* **2015**, *5*, 35608–35621; b) B. Badhani, N. Sharma, R. Kakkar, *RSC Adv.* **2015**, *5*, 27540–27557; c) P. De, M. Baltas, F. Bedos-Belval, *Curr. Med. Chem.* **2011**, *18*, 1672–1703; d) P. Eleni, P. Aikaterini, F. Ioannis, H.-L. Dimitra, *Curr. Pharm. Biotechnol.* **2018**, *19*, 1019–1048.
[7] a) G. Fitzl, L. Beyer, J. Sieler, R. Richter, J. Kaiser, E. Hoyer, *Z. Anorg. Allg. Chem.* **1977**, *433*, 237–241; b) R. Richter, L. Beyer, J. Kaiser, *Z. Anorg. Allg. Chem.* **1980**, *461*, 67–73; c) P. Knuuttila, H. Knuuttila, H. Hennig, L. Beyer, *Acta Chem. Scand.* **1982**, *36*, 541–545; d) J. Sieler, R. Richter, E. Hoyer, L. Beyer, O. Lindqvist, L. Andersen, *Z. Anorg. Allg. Chem.* **1990**, *580*, 167–174; e) W. Bensch, M. Schuster, *Z. Anorg. Allg. Chem.* **1992**, *615*, 93–96; f) W. Bensch, M. Schuster, *Z. Kristallogr. Cryst. Mater.* **1995**, *210*, 68–68; g) H. H. Nguyen, U. Abram, *Inorg. Chem.* **2007**, *46*, 5310–5319; h) H. Mandal, D. Ray, *Inorg. Chim. Acta* **2014**, *414*, 127–133; i) I. Barnard, K. R. Koch, *Inorg. Chim. Acta* **2019**, *495*, 119019.
[8] a) K. R. Koch, *Coord. Chem. Rev.* **2001**, *216–217*, 473–488; b) A. Saeed, U. Flörke, M. F. Erben, *J. Sulfur Chem.* **2014**, *35*, 318–355; c) A. Saeed, R. Qamar, T. A. Fattah, U. Flörke, M. F. Erben, *Res. Chem. Intermed.* **2017**, *43*, 3053–3093; d) A. Saeed, M. N. Mustafa, M. Zain-ul-Abideen, G. Shabir, M. F. Erben, U. Flörke, *J. Sulfur Chem.* **2019**, *40*, 312–350.
[9] a) A. Saeed, A. Mumtaz, H. Ishida, *J. Sulfur Chem.* **2011**, *32*, 45–54; b) A. Saeed, U. Shaheen, U. Florke, *Acta Crystallogr. Sect. E* **2010**, *66*, o1133; c) S. Gruschinski, A. Rodenstein, *Z. Anorg. Allg. Chem.* **2012**, *638*, 1179–1186.
[10] a) A. E. Dixon, J. Taylor, *J. Chem. Soc. Trans.* **1908**, *93*, 18–30; b) I. B. Douglass, F. B. Dains, *J. Am. Chem. Soc.* **1934**, *56*, 719–721.
[11] S. Behrendt, L. Beyer, F. Dietze, E. Kleinpeter, E. Hoyer, E. Ludwig, E. Uhlemann, *Inorg. Chim. Acta* **1980**, *43*, 141–144.
[12] a) L. R. Gomes, L. M. N. B. F. Santos, J. A. P. Coutinho, B. Schroder, J. N. Low, *Acta Crystallogr. Sect. E* **2010**, *66*, o870; b) H. Perez, R. S. Correa, A. M. Plutin, A. Alvarez, Y. Mascarenhas, *Acta Crystallogr. Sect. E* **2011**, *67*, o647; c) R. R. Cairo, A. M. P. Stevens, T. D. de Oliveira, A. A. Batista, E. E. Castellano, J. Duque, D. B. Soria, A. C. Fantoni, R. S. Corrêa, M. F. Erben, *Spectrochim. Acta A Mol. Biomol. Spectrosc.* **2017**, *176*, 8–17.
[13] H. A. Nkabyo, I. Barnard, K. R. Koch, R. C. Luckay, *Coord. Chem. Rev.* **2021**, *427*, 213588.
[14] a) H. Arslan, N. Külcü, U. Flörke, *Transition Met. Chem.* **2003**, *28*, 816–819; b) H. Arslan, U. Flörke, N. Külcü, M. F. Emen, *J. Coord.*

Chem. **2006**, *59*, 223–228; c) Y.-M. Zhang, H.-X. Pang, C. Cao, T.-B. Wei, *J. Coord. Chem.* **2008**, *61*, 1663–1670; d) H. Pérez, B. O'Reilly, A. M. Plutín, R. Martínez, R. Durán, I. G. Collado, Y. P. Mascarenhas, *J. Coord. Chem.* **2011**, *64*, 2890–2898.

[15] a) Z. Weiqun, Y. Wen, X. Liqun, C. Xianchen, *J. Inorg. Biochem.* **2005**, *99*, 1314–1319; b) H. Perez, Y. Mascarenhas, A. M. Plutin, R. d Souza Correa, J. Duque, *Acta Crystallogr. Sect. E* **2008**, *64*, m503; c) N. Gunasekaran, P. Jerome, S. W. Ng, E. R. T. Tiekink, R. Karvembu, *J. Mol. Catal. A* **2012**, *353–354*, 156–162; d) S. S. Tan, A. A. Al-abbasi, M. I. Mohamed Tahir, M. B. Kassim, *Polyhedron* **2014**, *68*, 287–294.

[16] A. Irving, K. R. Koch, M. Matoetoe, *Inorg. Chim. Acta* **1993**, *206*, 193–199.

[17] W. Yang, H. Liu, M. Li, F. Wang, W. Zhou, J. Fan, *J. Inorg. Biochem.* **2012**, *116*, 97–105.

[18] a) W. Hernández, E. Spodine, L. Beyer, U. Schröder, R. Richter, J. Ferreira, M. Pavani, *Bioinorg. Chem. Appl.* **2005**, *3*, 712186; b) X.-C. Huang, M. Wang, Y.-M. Pan, G.-Y. Yao, H.-S. Wang, X.-Y. Tian, J.-K. Qin, Y. Zhang, *Eur. J. Med. Chem.* **2013**, *69*, 508–520; c) İ. Koca, A. Özgür, M. Er, M. Gümüş, K. Açikalin Coşkun, Y. Tutar, *Eur. J. Med. Chem.* **2016**, *122*, 280–290; d) X.-E. Duan, R. Li, H.-B. Tong, Y.-Q. Li, S.-D. Bai, Y.-J. Guo, D.-S. Liu, *New J. Chem.* **2017**, *41*, 3333–3343.

[19] a) N. Selvakumaran, S. W. Ng, E. R. T. Tiekink, R. Karvembu, *Inorg. Chim. Acta* **2011**, *376*, 278–284; b) N. Selvakumaran, A. Pratheepkumar, S. W. Ng, E. R. T. Tiekink, R. Karvembu, *Inorg. Chim. Acta* **2013**, *404*, 82–87; c) N. Selvakumaran, N. S. P. Bhuvanesh, A. Endo, R. Karvembu, *Polyhedron* **2014**, *75*, 95–109; d) M. K. Rauf, S. Yaseen, A. Badshah, S. Zaib, R. Arshad, D. Imtiaz ud, M. N. Tahir, J. Iqbal, *JBIC J. Biol. Inorg. Chem.* **2015**, *20*, 541–554; e) N. Selvakumaran, L. Sandhiya, N. S. P. Bhuvanesh, K. Senthilkumar, R. Karvembu, *New J. Chem.* **2016**, *40*, 5401–5413; f) S. Yaseen, M. K. Rauf, S. Zaib, A. Badshah, M. N. Tahir, M. I. Ali, D. Imtiaz ud, M. Shahid, J. Iqbal, *Inorg. Chim. Acta* **2016**, *443*, 69–77; g) T. Yeşilkaynak, H. Muslu, C. Özpınar, F. M. Emen, R. E. Demirdöğen, N. Külcü, *J. Mol. Struct.* **2017**, *1142*, 185–193.

[20] C. Nguyen Thi Thanh, M. Truong Thi Cam, T. Pham Van, L. Nguyen, M. Nguyen Ha, L. Van Meervelt, *Acta Crystallogr. Sect. C* **2017**, *73*, 1030–1037.

[21] a) C. Liu, M. Wang, T. Zhang, H. Sun, *Coord. Chem. Rev.* **2004**, *248*, 147–168; b) T. Niittymäki, H. Lönnberg, *Org. Biomol. Chem.* **2006**, *4*, 15–25.

[22] J. Ye, P. Abiman, A. Crossley, J. H. Jones, G. G. Wildgoose, R. G. Compton, *Langmuir* **2010**, *26*, 1776–1785.

[23] a) Bruker, APEX2, 2014, Bruker AXS Inc., Madison, Wisconsin, USA; b) Bruker, SAINT, 2013, Bruker AXS Inc., Madison, Wisconsin, USA.

[24] a) G. Sheldrick, *Acta Crystallogr. Sect. A* **2015**, *71*, 3–8; b) G. Sheldrick, *Acta Crystallogr. Sect. C* **2015**, *71*, 3–8.

[25] O. V. Dolomanov, L. J. Bourhis, R. J. Gildea, J. A. K. Howard, H. Puschmann, *J. Appl. Crystallogr.* **2009**, *42*, 339–341.

Manuscript received: February 22, 2021
Revised manuscript received: April 4, 2021

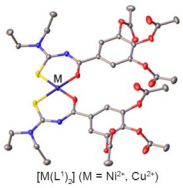

$[M(L^1)_2]$ (M = Ni^{2+}, Cu^{2+})

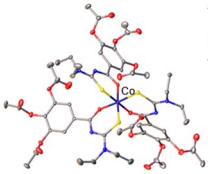

$[Co(L^1)_3]$

Tested compounds	IC_{50} /μM	
	MCF7	HepG2
HL^1	70.17 ± 5.80	97.63 ± 9.65
$[Ni(L^1)_2]$	64.84 ± 6.94	89.42 ± 2.20
$[Cu(L^1)_2]$	94.21 ± 2.46	113.2 ± 1.14
$[Co(L^1)_3]$	22.23 ± 1.58	28.30 ± 3.09
cisplatin	45.7 ± 1.2	13.3 ± 1.1

Prof. Dr. C. Thang Pham, T. Thuy Pham, V. Ha Nguyen, Prof. Dr. T. Nguyet Trieu, Prof. Dr. H. Huy Nguyen**